A porcine in-vivo model of acute pulmonary embolism

Schultz, Jacob; Andersen, Asger; Gade, Inger-Lise; Ringgaard, Steffen; Kjaergaard, Benedict; Nielsen-Kudsk, Jens Erik

Published in:
Pulmonary Circulation

DOI (link to publication from Publisher):
10.1177/2045893217738217

Publication date:
2018

Document Version
Publisher's PDF, also known as Version of record

Research Article

Pulmonary Circulation

A porcine *in-vivo* model of acute pulmonary embolism

Jacob Schultz[1], Asger Andersen[1], Inger Lise Gade[2], Steffen Ringgaard[3], Benedict Kjaergaard[4] and Jens Erik Nielsen-Kudsk[1]

[1]Department of Cardiology, Aarhus University Hospital, Aarhus, Denmark; [2]Department of Clinical Medicine, Aalborg University, Aalborg, Denmark; [3]The MR Centre, Aarhus University Hospital, Aarhus, Denmark; [4]Department of Thoracic Surgery, Aalborg University Hospital, Aalborg, Denmark

Abstract

Acute pulmonary embolism (PE) is the third most common cardiovascular cause of death after acute myocardial infarction and stroke. Patients are, however, often under-treated due to the risks associated with systemic thrombolysis and surgical embolectomy. Novel pharmacological and catheter-based treatment strategies show promise, but the data supporting their use in patients are sparse. We therefore aimed to develop an in vivo model of acute PE enabling controlled evaluations of efficacy and safety of novel therapies. Danish Landrace pigs ($n = 8$) were anaesthetized and mechanically ventilated. Two pre-formed autologous PEs (PE1, PE2, 20×1 cm) were administered consecutively via the right external jugular vein. The intact nature and central location were visualized in situ by magnetic resonance imaging (MRI). The hemodynamic and biochemical responses were evaluated at baseline (BL) and after each PE by invasive pressure measurements, MRI, plus arterial and venous blood analysis. Pulmonary arterial pressure increased after administration of the PEs (BL: 16.3 ± 1.2, PE1: 27.6 ± 2.9, PE2: 31.6 ± 3.1 mmHg, BL vs. PE1: $P = 0.0027$, PE1 vs. PE2: $P = 0.22$). Animals showed signs of right ventricular strain evident by increased end systolic volume (BL: 60.9 ± 5.1, PE1: 83.3 ± 5.0, PE2: 99.4 ± 6.5 mL, BL vs. PE1: $P = 0.0005$, PE1 vs. PE2: $P = 0.0045$) and increased plasma levels of Troponin T. Ejection fraction decreased (BL: 58.9 ± 2.4, PE1: 46.4 ± 2.9, PE2: 37.3 ± 3.5%, BL vs. PE1: $p = 0.0008$, PE1 vs. PE2: $P = 0.009$) with a compensatory increase in heart rate preserving cardiac output and systemic blood pressure. The hemodynamic and biochemical responses were comparable to that of patients suffering from intermediate-high-risk PE. This porcine model mirrors the anatomical and physiologic changes seen in human patients with intermediate-high-risk PE, and may enable testing of future therapies for this disease.

Keywords

animal models, magnetic resonance imaging, catheterization, pig

Date received: 3 July 2017; accepted: 1 October 2017

Pulmonary Circulation 2017; 8(1) 1–9

DOI: 10.1177/2045893217738217

Acute pulmonary embolism (PE) is a common disease with a high mortality, making it the third most common cardiovascular cause of death, surpassed only by acute myocardial infarction and stroke.[1,2]

To optimize treatment, patients with acute PE are stratified into groups of low-risk, intermediate-low-risk, intermediate-high-risk, and high-risk of early mortality based on clinical presentation, measures of right ventricular (RV) strain, and systemic hemodynamic impairment. Cornerstones in the treatment are anticoagulation therapy in low-risk and intermediate-low-risk patients and thrombolytic therapy in high-risk patients.[3–5] However, thrombolysis is contraindicated in one-third of the high-risk patients due to the increased risk of bleeding.[6] Even in patients screened

Corresponding author:
Jacob Schultz, Department of Cardiology – Research, Aarhus University Hospital Palle Juul-Jensens Boulevard 99, 8200 Aarhus, Denmark.
Email: jacobgschultz@clin.au.dk

for contraindications, systemic thrombolysis is associated with a 3% risk of stroke and 13% risk of major bleeding.[7] Today, the alternate treatment is emergency surgical embolectomy, but co-morbidities often make these patients poor candidates for major surgery, indicated by in-hospital mortality rates at 30% for the procedure.[8]

The development of new treatment strategies is ongoing. Newly developed catheter-directed therapies have shown promise as a new treatment option by enabling effective thrombus removal without the risks associated with standard treatment.[9,10] Strategies of pharmacological unloading and support of the RV during acute PE has also shown promise.[11,12] However, data supporting the use of these novel treatment options in patients are sparse. Due to the heterogeneous and acute nature of the disease, large clinical trials are challenging to conduct. To investigate the efficacy and safety of these novel pharmacological and catheter-based treatment options, thorough controlled preclinical studies are needed.

The majority of current experimental models of PE are ex vivo.[13] To evaluate efficacy and safety of novel treatments in a setting comparable to human physiology, larger in vivo animal models are needed. Such a model would need to be comparable to the clinical presentation of patients suffering from intermediate-risk or high-risk PE as these risk groups are the main candidates for new treatments. Furthermore, the embolus should be of autologous blood to enable evaluation of thrombolytic agents. To mimic the event of a large centrally located PE (the type of PE most suitable for catheter-based interventions), the thrombus needs to be large enough to lodge in the main pulmonary arteries. Finally, the model needs to be well characterized regarding RV function, systemic hemodynamics, biochemical responses, visualization of emboli sms in situ, and preferably allow for serial evaluations. There are overall very few in vivo models of acute PE and, to our knowledge, none that fulfills all of the criteria above.[14–22]

We aimed to develop and characterize a model of centrally located autologous intermediate-high-risk PE in pigs suitable for evaluation of novel catheter and pharmacological therapies.

Methods

Animals

The study was approved by the Danish Animal Research Inspectorate (license number: 2016-15-0201-00840) and was conducted in accordance with institutional and national guidelines for the ethical care of animals. Eight female Danish Landrace pigs (~60 kg) were used. Animals were housed, handled, and transported according to the guidelines of the Danish Animal Research Inspectorate.

Criteria

The aim of this study was to develop a model of intermediate to high-risk acute PE, as defined according to the European Society of Cardiology guidelines.[3] The following criteria needed to be met: hemodynamic and biochemical signs of RV strain with a preserved systemic circulation characterized by increased pulmonary artery pressures (PAP); RV dilatation; decreased right ventricular ejection fraction (RVEF); increased plasma levels of Troponin T (TnT); but unchanged cardiac output (CO) and systolic blood pressure. Second, to enable evaluations of catheter directed therapies, the PE should remain intact after administration and be visualized in situ in the central pulmonary arteries by magnetic resonance imaging (MRI).

Study design

Two consecutive PEs were administered to eight Danish Landrace pigs (PE1 and PE2). All animals followed the same protocol (Fig. 1) and served as their own controls. Approximately 150 min after induction of anesthesia, baseline (BL) measurements were performed outside the MRI scanner: ventilator settings and output were noted. Invasive systemic blood pressures and heart rate were noted. Venous and arterial blood samples were drawn and transferred to the lab immediately. A right heart catheterization (RHC) was performed, guided by continuous pressure wave monitoring. Due to the slight magnetic properties of the Swan-Ganz catheter, it was removed before the flat bed was positioned in the scanner. Heart and lung MRI

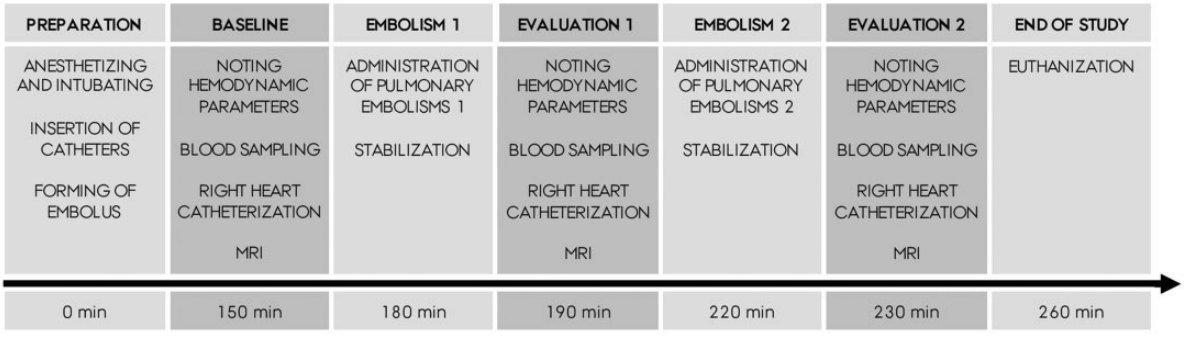

Fig. 1. Study design (n = 8).

scans were then performed. The duration of the evaluation process was approximately 30 min. At 180 min, PE1 was administered. After allowing for stabilization for 10 min, the evaluation process was repeated. At 220 min, PE2 was administered and at 230 min, the final evaluation was performed. The pig was euthanized with an intravenous (IV) injection of Pentobarbital (67 mg/kg, Exagon® vet, Richter Pharma, Austria).

Anesthesia, instrumentation, and invasive pressures

The pigs were premedicated by subcutaneous injections of Azaperone (2.2 mg/kg, Stesnil®, Elanco, USA) and Midazolam (0.5 mg/kg, Hameln Pharma, Germany) before transport to the research facilities. Upon arrival, an IV access was obtained in a vein on the ear. Anesthesia was induced with an IV bolus injection of Etomidate (0.5 mg/kg, Hypnomidate®, Janssen Pharmaceutical, Belgium) and maintained with continuous IV infusion of Fentanyl (5 µg/kg/h, Hameln Pharma, Germany) and Propofol (2 mg/kg/h, Propolipid, Fresnius Kabi, Germany). The pigs were intubated (ID 7.5 mm, Unomedical, Malaysia) and ventilated by a mechanical ventilator with tidal volume 8 mL/kg, respiratory rate 16 breaths/min (adjusted to achieve an end tidal CO2 [ETCO2] 5.0–5.5) and no positive end-expiratory pressure. The fraction of inspired oxygen was initially set to 1.0 to compensate for the hypoxia during intubation, but reduced to 0.3 after stabilization to mimic room air. All ventilation settings were maintained unchanged throughout the experiment. A pulse oximeter was attached to the ear to monitor oxygen saturation. A bladder catheter (size 14) was inserted to collect urine. To ensure normothermia, the pig was covered with a warming blanket (Bair Hugger, 3M, MN, USA) and the temperature monitored by a rectal thermometer.

All vascular accesses were obtained using an ultrasound-guided minimal-invasive approach. A 17-gauge Venflon cannula was used for vessel puncture to enable the introduction of a guidewire. A small incision was made at the level of the skin before a sheath was introduced over the wire. To avoid interfering with the coagulation system, no heparin was used. Instead, all vascular accesses were flushed regularly with isotonic saline to avoid clotting. Three sheaths were inserted. A 7-French (F) sheath was inserted in the left external jugular vein for drawing of blood for the emboli and for serial blood sampling. A 6-F sheath was inserted in the left femoral artery for measurement of arterial blood pressure and for serial arterial blood sampling. A 26-F Dry-Seal sheath (Gore Medical, USA) was inserted in the right external jugular vein guided by fluoroscopy. A 1.5-cm incision was made in the skin and the underlying musculature, before the vessel was dilated with a 12-F sheath. The 26-F Dry-Seal sheath was introduced over the wire (Amplatz extra stiff, 0.035'', Mermaid Medical, Denmark) to the superior vena cava at the level of the right atrium. Additional to administration of emboli, the dry-seal port was used for insertion of a Swan-Ganz catheter (7.5F, CCOmbo, Edwards Lifescience, USA). RHCs were performed using standard techniques. To avoid manipulating or fragmenting the embolus or placing the catheter in an obstructed segment hereby obtaining incorrect values, the catheter was placed in the main pulmonary artery (PA) and we did not perform wedging.

Creation and administering of pulmonary emboli

The emboli were created ex vivo using an autologous blood sample. Immediately after achieving venous access 120 mL blood was drawn (replaced with 120 mL of isotonic saline). Then, 30 mL blood was injected into 4.75″ plastic tubes (only two were used, the other two served as a reserve). A total of 0.1 mL gadolinium contrast (279.3 mg/mL, Dotarem®, Guerbet, France) was added and the tubes were clamped at both ends to mix the gadolinium in the blood. After hanging vertically for 3–4 h at room temperature, the samples divided into two phases: the supernatant and the embolus. The supernatant was discarded and the embolus placed on a clean swap to dry of excess fluids. As we suspended the blood at a vertical position, the thrombus took shape after the longitudinal cylindrical tube. By this protocol, we were able to create very consistent cylindrical emboli (1 × 20 cm) mimicking those that could be dislodged in relation to deep venous thrombosis (Fig. 2). For administering, the embolus was transferred to another tube and suspended in isotonic saline. This tube was connected to a 26-F Dry-Seal sheath in the right external jugular vein via a cannula. A pressure bag with isotonic saline (200 mmHg) was attached to the distal end of the tube and the system

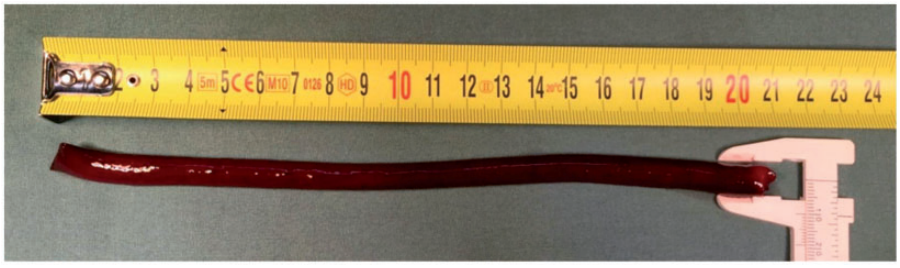

Fig. 2. Embolus. Photo illustrating a representative example of an embolus with rulers showing a diameter of 1 cm and length of 20 cm.

was filled and emptied of air (Fig. 3, Video 1). When in place, the saline flow carried the embolus en bloc through the cannula, via the sheath to the right atrium. Afterwards the saline flow was stopped and the cannula removed. The embolus was then carried by the blood flow from the right atrium, via the RV, to the PA and lodged as a PE. All isotonic saline used for flushing, replacing of blood loss, and infusion of anesthesia were recorded.

Magnetic Resonance Imaging

MRI was performed with a 1.5-T whole-body scanner (Achieva dStream, Philips, Best, The Netherlands). Animals were transported to the scanner with manual ventilation. The ventilator and infusion pumps were placed in the control room and connected to the pig via tube extension. An electrocardiogram as well as respiratory rate was measured continuously to enable precise triggering. By maintaining the exact location of pig on the flat bed, we were able to use unaltered MRI projections enabling precise serial measuring. Total scan time for all sequences after injection of the embolus was about 20 min.

Functional measures

All functional scans were performed at BL and after each of the emboli. To measure RVEF as well as the volume of the right and left ventricle, a stack with 14 slices of cine acquisitions, encompassing the heart from base to apex in the cardiac short-axis orientation, was acquired. A balanced steady-state-free-precession (B-SSFP) pulse sequence was used with a field of view (FOV) of 300 × 300 mm, acquisition matrix of 152 × 155, slice thickness was 8 mm, and 30 heart phases were acquired. To measure flow, right ventricular stroke volume (RVSV), and cardiac output, a phase contrast sequence was obtained from the RV outflow tract. FOV was 350 × 350 mm, acquisition matrix was 288 × 288, slice thickness was 8 mm, and the velocity encoding parameter (Venc) was 100 cm/s. All image analyses of functional parameters were performed using the freely available software Segment 2.0 (Medviso, http://segment.heiberg.se). Volumes of the RV was measured by manually drawing the endocardium during end-diastole and end-systole on all slices encompassing the heart. By drawing a region of interest at the cross-sectioned PA in the phase-contrast scan, pulmonary flow curves were obtained. After adjusting for eddy currents, RVSV and CO were calculated. All analyses were performed by a trained blinded investigator.

Pulmonary angiography

At BL, a three-dimensional (3D) B-SSFP scan was acquired in the diastole to visualize the pulmonary vasculature. Slice thickness was 3 mm, FOV was 360 × 360 × 200 mm, and matrix was 256 × 256 × 66. To obtain images of the emboli in situ, 3D diastolic scans with an inversion pulse (same parameters as above) were performed both at BL and following injection of each embolus. To determine the optimal inversion time, we performed a Look-Locker T1 mapping. We chose the inversion time with the lowest signal for blood. At this time, a weak signal was obtained from the myocardium, while the emboli, containing Gadolinium, showed a

Fig. 3. Experimental set-up. A pig is lying on the flat bed in the MRI scanner. It is wrapped in plastic to avoid risk of contaminating the scanner. On top of the pig is the coil. On the green cloth is the tube with the PE suspended in saline (black arrow). Attached are the cannula with a plastic clamp (white arrow) and the MRI-safe pressure bag (dashed white arrow).

high signal. A two-dimensional respiration navigator method was used enabling scanning during free-breathing.[23] Image analyses were performed using OsiriX (Pixmeo SARL, Switzerland). The BL 3D scan with inversion pulse was subtracted from the post-emboli scan, leaving only the emboli. This scan was then merged with the BL 3D scan enabling a 3D visualization of the emboli in situ.

Biochemical analyses

At each point of evaluation, a venous and arterial blood sample was drawn and transported to the lab within 5 min. The arterial sample was analyzed for partial pressures of blood gasses and concentrations of electrolytes, lactate, and glucose (ABL90 FLEX PLUS, Radiometer Medical, Denmark). The venous blood sample was drawn in Lithium Heparin tubes, centrifuged at 5000 RPM for 10 min at 4°C. Plasma was then collected and placed at −20°C. Plasma samples were analyzed for levels of TnT, a biomarker of RV strain, by a blinded investigator at the Department of Clinical Biochemistry at Aarhus University Hospital using a high sensitivity assay (Elecsys, Roche, Basel, Switzerland). The predetermined cut-off value determined by the manufacturer and validated in a large multicenter cohort of patients with acute PE.[24]

Statistics

The study was designed as repeated measures with a within-subject variable. Each animal therefore served as its own control. We used an ANOVA model with paired multiple comparisons to test for mean differences between variables: BL vs. PE1 and PE1 vs. PE2. Shapiro Wilks normality test was used to test for normal distribution. Normally distributed data are presented as mean ± standard error of mean (SEM). $P < 0.05$ were considered significant.

Results

Visualization of pulmonary embolism in situ

We obtained pulmonary angiographies at BL and after each embolus by MRI and found that the emboli reached the pulmonary vasculature without fragmenting (2/16 PEs did fragment into smaller emboli, though still lodging centrally). Emboli lodged centrally as either a saddle embolus (n = 3), in the right PA (n = 8) or left PA (n = 5), and stretched down to the segmental arteries (Fig. 4, Videos 2 and 3). Seven of eight pigs had bilateral PEs. For a description of the location of each PE see supplement (Table 1).

Hemodynamic signs of RV strain

PAPs increased twofold after administering the PEs (Fig. 5), indicating a substantial increase in afterload. The RV showed signs of strain after PE1 and even further after PE2 as seen by increasing right ventricular end-diastolic (RVEDV) and right ventricular end-systolic volumes (RVESV) and with RVSV. This translated into a considerable decrease in RVEF (Fig. 5). A compensatory increase in heart rate, however, prevented impairment of the systemic circulation evident by an unaltered CO and systemic mean arterial blood pressure (MAP) (Fig. 5). Despite an unaltered MAP, we did observe an increase in diastolic blood pressure after PE1 (mmHg, BL: 53.3 ± 3.8 vs. PE1: 59.1 ± 2.6, $P = 0.043$) and a decline in pulse pressure with PE1 and PE2 (mmHg, BL: 57.6 ± 4.4, PE1: 52.0 ± 6.6, PE2: 46.4 ± 7.7, $F(1.88,13.2) = 5.28$, $P = 0.02$). This corresponded well with the decreased RVSV measured by MRI.

Biochemical signs of RV strain

Plasma levels of TnT were elevated after PE1 compared to BL (Fig. 6). After PE2, the concentration of TnT

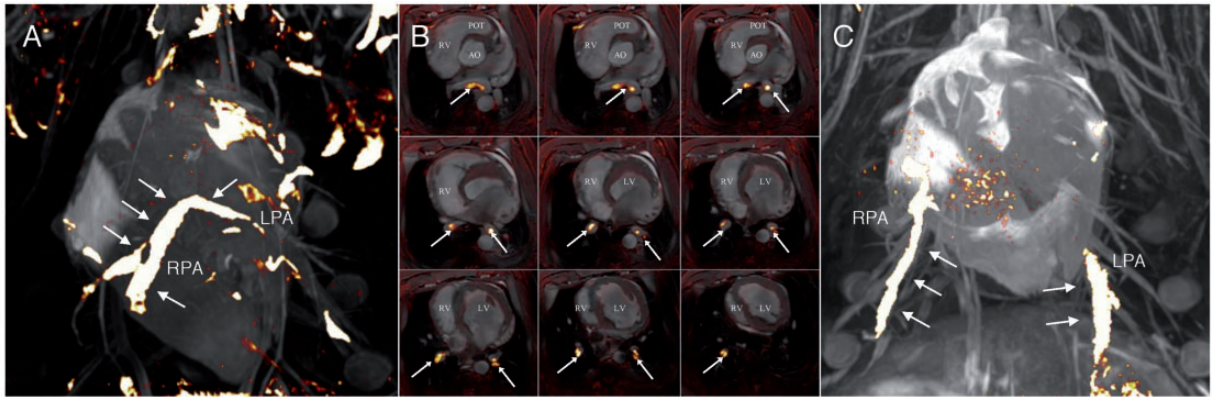

Fig. 4. 3D MRI of pulmonary emboli in situ. (a) 3D MRI image illustrating a saddle embolus in situ. Notice that the embolus is still intact and hinged on the pulmonary bifurcation. (b) Images depict a saddle embolus on slices from the main PA (top left) to the distal segmental arteries (low right). (c) 3D MRI image illustrating bilateral PEs. Pes are colored yellow with white arrows.
LV, left ventricle; RV, right ventricle; Ao, aorta; POT, pulmonary outflow tract; RPA, right pulmonary artery; LPA, left pulmonary artery.

Table 1. Location of PE in situ.

Animal	PE1	PE2	Bilateral
1	RPA to distal segmental arteries	LPA to distal segmental arteries	Yes
2	LPA to distal segmental arteries	Right lower segmental arteries; fragmented	Yes
3	RPA to both upper and lower RPA.	Saddle to both RPA and LPA	Yes
4	Saddle to both RPA and LPA	RPA to both upper and lower RPA	Yes
5	RPA to lower segmental arteries	LPA to both upper and lower LPA	Yes
6	RPA to lower segmental arteries	LPA to lower segmental arteries	Yes
7	Left lower segmental arteries; fragmented	Saddle to both RPA and LPA	Yes
8	Lower right segmental arteries	RPA stretching to both upper and lower RPA	No

RPA, right pulmonary artery; LPA, left pulmonary artery.

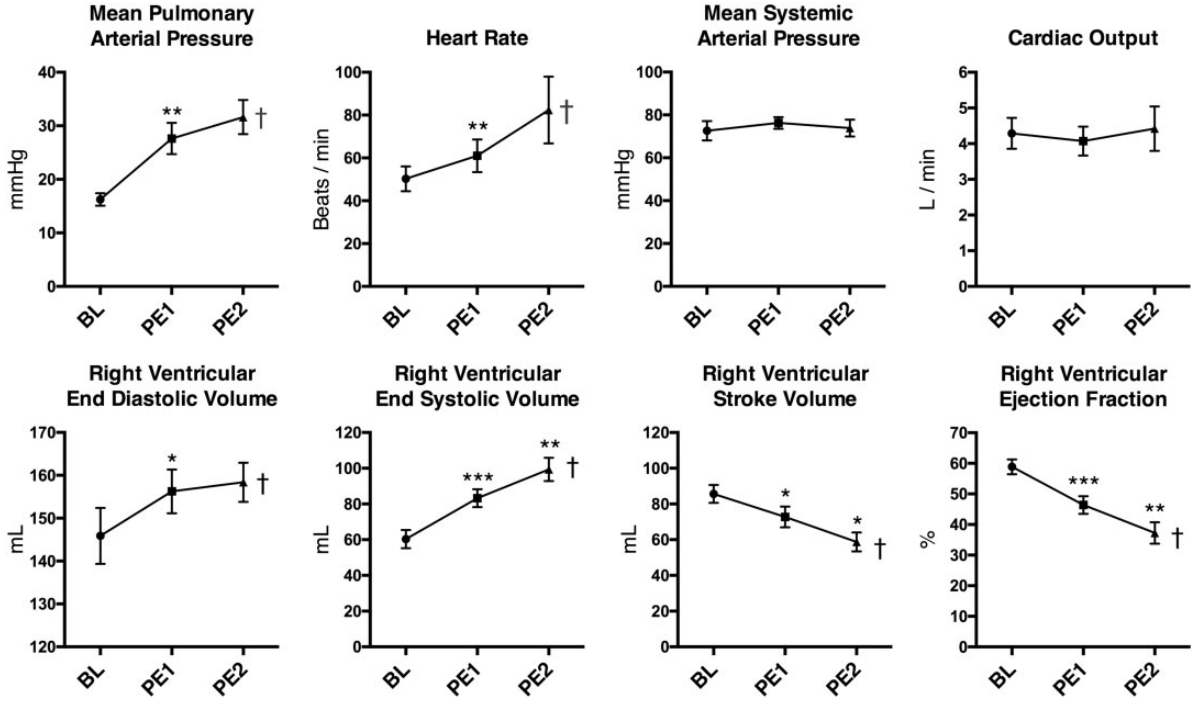

Fig. 5. Hemodynamic signs of RV strain. Data presented as mean ± SEM. $^{*}P < 0.05$, $^{\dagger}P < 0.05$ for Anova analyses.

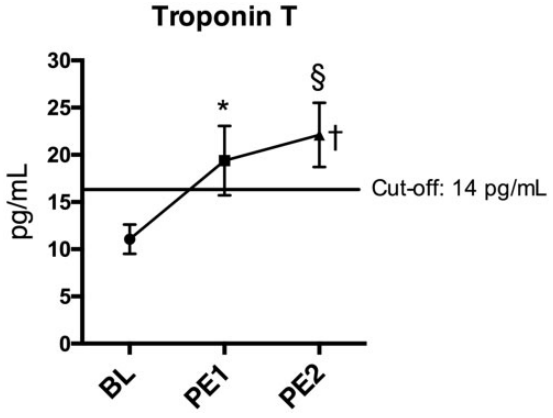

Fig. 6. Biochemical signs of RV strain. Data presented as mean ± SEM. $^{*}P < 0.05$, $^{\dagger}P < 0.05$ for Anova analyses, $^{\S}P$ (one-sided) < 0.05 vs. cut-off 14 pg/mL.

surpassed the validated cut-off value for RV strain of 14 pg/mL (Fig. 6).

Gas exchange

As the ventilation settings were maintained constant throughout the experiment, the animals were unable to increase their ventilation minute volume in contrast to a patient suffering from acute PE. While a constant minute volume is not the normal physiological response, it allowed us to indirectly evaluate the ventilation/perfusion mismatch by the impaired gas exchange. $ETCO_2$ was monitored during the administering of the emboli. We found that the $ETCO_2$ decreased immediately after each embolus, but within minutes it increased to levels even higher than BL. We noted that the minimum value decreased with each

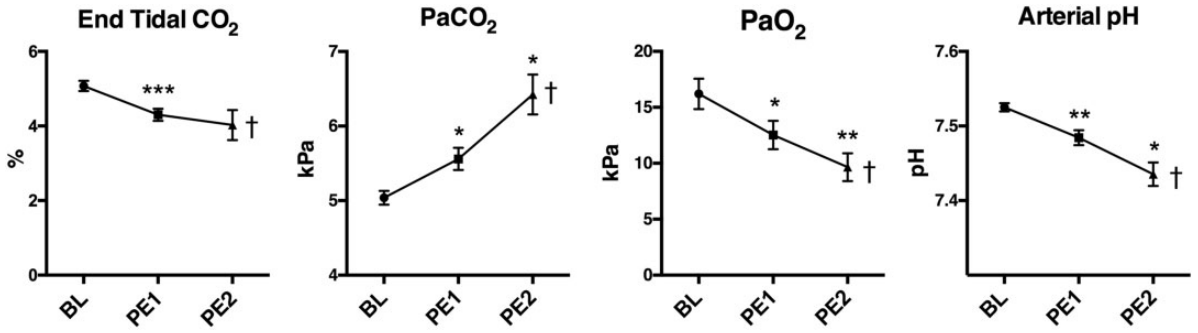

Fig. 7. Gas exchange. Data presented as mean ± SEM. $^{*}P < 0.05$, $^{\dagger}P < 0.05$ for Anova analyses.

embolus (Fig. 7). Partial arterial CO_2 pressure increased significantly while partial arterial O_2 pressure decreased. Taken together this corresponds well with an increasing ventilation/perfusion mismatch causing an accumulation of arterial CO_2. This caused a respiratory acidosis as seen by the decreasing arterial pH (Fig. 7).

Discussion

By administering two consecutive PEs in an in vivo porcine model, we found a dose-dependent increase in both hemodynamic and biochemical signs of RV strain with preserved systemic circulation. The response of the animals to the PEs was comparable to what is found for patients suffering from intermediate-high-risk PE.[3]

To our knowledge, this is the first model to successfully visualize an autologous contrast-enhanced PE by MRI. This enables us to confirm the intact nature and central location of the emboli in our model. For further interventional studies in this model, the in situ visualization may prove important as it provides a precise evaluation of the degree of residual emboli.

We aimed to develop a model of acute PE comparable to intermediate-high-risk PE in patients. We found that the injection of one embolus indeed caused RV strain comparable to that of intermediate-risk patients. PAPs increased causing the RV to dilate. Despite the finding of a decrease in RVSV and RVEF, CO was maintained by a compensatory increase in heart rate. This physiological response is similar to what is seen in patients suffering from intermediate-risk PE. In high-risk patients, however, the RV is unable to overcome the afterload by increasing contractility and heart rate; hence, CO and systemic blood pressure will decrease. In current guidelines, systemic hypotension or shock is therefore the criterion that differentiates high-risk patients from patients at intermediate-risk of early death. While the PAPs and RV strain increased further after the second embolus in our model, the systemic circulation remained uncompromised. Despite a further increase in heart rate, the animals did not develop systemic hypotension. The animals did, however, show biochemical signs of RV strain with levels of TnT above the cut-off value, making the model comparable to patients suffering from intermediate to high-risk PE.[3] The pigs compensated well, even when challenged by a massive thrombus burden. It is well-known that the thrombus burden alone does not define the outcome of a patient suffering from acute PE. Two patients exposed to the same thrombus burden may show very different clinical responses depending on their RV function. A PE of a given size can be fatal in an elderly patient with co-morbidity, but may only cause mild symptoms in a young and fit person. The fact that we have used young and previously healthy animals may be a reason why they did not show signs of compromised systemic circulation. In pilot studies, we attempted to administer a third embolus, but found it to cause uncontrollable hemodynamic collapse and death. This underlines the narrow interval between high-risk PE and fatal PE. A stable model of high-risk PE in pigs with an acceptable variance and mortality rate may therefore be difficult to develop.

This is, to our knowledge, the first experimental model of massive centrally located autologous PE. The majority of current experimental models of PE are ex vivo.[13] Ex vivo models are relevant for fast and cost-effective testing of novel treatment options in the early development phase. Before implementing new treatment strategies in patients, it is, however, pivotal to evaluate the efficacy and safety in a setting more comparable to human physiology. Larger animal models may provide this opportunity. The very few existing in vivo models use predominantly artificial materials such as plastic spheres or balloons to obstruct the PAs.[16–20] The evaluation of novel treatments including thrombolytics is therefore not possible in these models. Furthermore, the evaluation of catheter directed therapies would be questionable, as the material removed would differ significantly from a real embolus. A few models have used autologous thrombus made ex vivo as in our model.[14,15,21] However, emboli in these studies are much smaller in size, and though these studies have not described the location of the emboli in situ, we can presume that they would travel distally in the pulmonary circulation. These models may be suitable for evaluation of pharmacological treatment, while a more proximal location of the emboli would be more suited for the evaluation of catheter-directed therapies. The autologous nature, the central location and the in situ visualization of the PE, makes our model suitable for the

evaluation of a wide range of therapies. Furthermore, the very comprehensive and precise hemodynamic characterization of the model ensures a controlled and sensitive evaluation.

Limitations

The model is indeed an animal model and we cannot rule out inter-species differences. The pig has, however, previously proven a valid species for translatable cardiovascular models due to its anatomy, size and hemodynamics.

Despite achieving an autologous embolus with a size and shape similar to that in patients, it was however still created ex vivo. Emboli in patients are often formed in the lower extremity veins where it is exposed to continuous substrates and inflammatory components. A recent study compared ex vivo thrombi with thrombi from thrombectomies and found the latter to be more heterogeneous and contain more extracellular matrix.[25] The same study, however, showed that adding thrombin did not increase the fraction of extracellular matrix. Therefore, we chose spontaneous coagulation in our model. Due to the homogeneous nature and low fraction of extracellular material of the embolus in this model we believe that it corresponds to a fresh thrombus in patients. As it was rigid and proved intact after injection, we find it suitable for evaluation of both catheter-based and fibrinolytic therapies. An experimental model of a more chronic thrombus created in vivo in the inferior vena cava has been developed.[22] In this chronic model, it was, however, not possible to control the size of the thrombus, thereby creating a large variance in the model. Furthermore, the model is time-consuming and logistically challenging.

We chose to use the combination of IV Fentanyl and Propofol as analgesia and anesthesia in this model. In pilot studies, we used inhaled Sevoflurane, but found that the inherent ventilation/perfusion mismatch caused by the emboli caused differences in anesthetic depth and introduced bias. We therefore chose IV infusions and found that the Propofol/Fentanyl combination in the lowest possible concentrations was the most stable option. We performed repeat measures and used the same low dose of IV anesthetics throughout the protocol to minimize bias. Hemodynamic measures may, however, be influenced by anesthesia which should be taken into consideration in the interpretation of the results from this study. We performed serial MRI scans in this protocol. This can be a challenge due to availability and cost. MRI, compared to the more traditional CT or echocardiography, however, provides important additional data. Most importantly, the phase-contrast images provide the golden standard of cardiac output measures, which is pivotal for the evaluations of the RV function.[26] Furthermore, the thin slices of the RV enable precise measures of RV volumes, important to determine RV strain. Finally, the novel 3D angiographies with contrast-enhanced emboli provides excellent images to determine the location of the emboli. In future studies using this model, echocardiography could potentially be an alternative to MRI where this modality is unavailable. One should, however, be aware of the challenges of performing trans-thoracic echocardiography in pigs. The pointed anatomy of the pig chest impairs the quality of obtained images significantly. Trans-esophageal echocardiography may, however, be an alternative to MRI.

Conclusion

We succeeded in developing an in vivo model of central autologous acute PE in pigs. To our knowledge, this is the first model to successfully visualize an autologous contrast-enhanced PE on MRI. By administering two consecutive PE, we found a dose-dependent increase in RV strain with preserved systemic circulation. The model is comparable to patients suffering from intermediate-high-risk PE and may prove a useful tool in the preclinical evaluation of novel catheter-directed and pharmacological therapies for these patients.

Acknowledgements

All experiments were performed at the Department of Cardiology and the Department of Clinical Medicine, Aarhus University Hospital, 8200 Arhus, Denmark.

Conflict of interest

The author(s) declare that there is no conflict of interest.

Funding

This work was supported by: Aarhus University Graduate School, The Novo Nordisk foundation (NNF16OC0023244), Holger og Ruth Hesses mindefond, Søster og Verner Lipperts Fond, Direktør Kurt Bønnelyckes fond.

References

1. Cohen AT, Agnelli G, Anderson FA, et al. Venous thromboembolism (VTE) in Europe. *The number of VTE events and associated morbidity and mortality*. Thromb Haemost 2007; 98: 756–764.
2. Goldhaber SZ and Bounameaux H. Pulmonary embolism and deep vein thrombosis. *Lancet* 2012; 379: 1835–1846.
3. Konstantinides SV, Agnelli G, et al.; Authors/Task Force Members. 2014 ESC Guidelines on the diagnosis and management of acute pulmonary embolism: The Task Force for the Diagnosis and Management of Acute Pulmonary Embolism of the European Society of Cardiology (ESC) * * Endorsed by the European Respiratory Society (ERS). *Eur Heart J* 2014; 35: 3033–3073.
4. Konstantinides S, Tiede N, Geibel A, et al. Comparison of alteplase versus heparin for resolution of major pulmonary embolism. *Am J Cardiol* 1998; 82: 966–970.
5. Goldhaber SZ, Haire WD, Feldstein ML, et al. Alteplase versus heparin in acute pulmonary embolism: randomised trial assessing right-ventricular function and pulmonary perfusion. *Lancet* 1993; 341: 507–511.

6. Stein PD and Matta F. Thrombolytic therapy in unstable patients with acute pulmonary embolism: saves lives but underused. *Am J Med* 2012; 125: 465–470.
7. Chatterjee S, Chakraborty A, Weinberg I, et al. Thrombolysis for pulmonary embolism and risk of all-cause mortality, major bleeding, and intracranial hemorrhage. *JAMA* 2014; 311: 2414.
8. Stein PD, Alnas M, Beemath A, et al. Outcome of pulmonary embolectomy. *Am J Cardiol* 2007; 99: 421–423.
9. Kuo WT, Gould MK, Louie JD, et al. Catheter-directed therapy for the treatment of massive pulmonary embolism: systematic review and meta-analysis of modern techniques. *J Vasc Interv Radiol* 2009; 20: 1431–1440.
10. Kucher N, Boekstegers P, Muller OJ, et al. Randomized, controlled trial of ultrasound-assisted catheter-directed thrombolysis for acute intermediate-risk pulmonary embolism. *Circulation* 2014; 129: 479–486.
11. Souza-Silva AR, Dias-Junior CA, Uzuelli JA, et al. Hemodynamic effects of combined sildenafil and l-arginine during acute pulmonary embolism-induced pulmonary hypertension. *Eur J Pharmacol* 2005; 524: 126–131.
12. Neto-Neves EM, Dias-Junior CA, Uzuelli JA, et al. Sildenafil improves the beneficial hemodynamic effects exerted by atorvastatin during acute pulmonary thromboembolism. *Eur J Pharmacol* 2011; 670: 554–560.
13. Biederer J, Charalambous N, Paulsen F, et al. Treatment of acute pulmonary embolism: local effects of three hydrodynamic thrombectomy devices in an ex vivo porcine model. *J Endovasc Ther* 2006; 13: 549–560.
14. Beam DM, Neto-Neves EM, Stubblefield WB, et al. Comparison of isoflurane and α-chloralose in an anesthetized swine model of acute pulmonary embolism producing right ventricular dysfunction. *Comp Med* 2015; 65: 54–61.
15. Kjærgaard B, Kristensen SR, Risom M, et al. A porcine model of massive, totally occlusive, pulmonary embolism. *Thrombosis Research* 2009; 124: 226–229.
16. Roehl AB, Steendijk P, Baumert JH, et al. Comparison of 3 methods to induce acute pulmonary hypertension in pigs. *Comp Med* 2009; 59: 280–286.
17. Kudlička J, Mlček M, Hála P, et al. Pig model of pulmonary embolism: where is the hemodynamic break point? *Physiol Res* 2013; 62(Suppl. 1): S173–179.
18. Tsang JYC, Lamm WJE, Starr IR, et al. Spatial pattern of ventilation-perfusion mismatch following acute pulmonary thromboembolism in pigs. *J Appl Physiol* 2005; 98: 1862–1868.
19. Dias-Junior CA and Tanus-Santos JE. Hemodynamic effects of sildenafil interaction with a nitric oxide donor compound in a dog model of acute pulmonary embolism. *Life Sci* 2006; 79: 469–474.
20. Böttiger BW, Motsch J, Dörsam J, et al. Inhaled nitric oxide selectively decreases pulmonary artery pressure and pulmonary vascular resistance following acute massive pulmonary microembolism in piglets. *Chest* 1996; 110: 1041–1047.
21. Pereira DJ, Moreira MM, Paschoal IA, et al. Near-fatal pulmonary embolism in an experimental model: hemodynamic, gasometric and capnographic variables. *Rev Bras Cir Cardiovasc* 2011; 26: 462–468.
22. Barbash IM, Schenke WH, Halabi M, et al. Experimental model of large pulmonary embolism employing controlled release of subacute caval thrombus in swine. *J Vasc Interv Radiol* 2011; 22: 1471–1477.
23. Henningsson M, Smink J, Razavi R, et al. Prospective respiratory motion correction for coronary MR angiography using a 2D image navigator. *Magn Reson Med* 2012; 69: 486–494.
24. Lankeit M, Jimenez D, Kostrubiec M, et al. Predictive value of the high-sensitivity troponin T assay and the simplified Pulmonary Embolism Severity Index in hemodynamically stable patients with acute pulmonary embolism: a prospective validation study. *Circulation* 2011; 124: 2716–2724.
25. Krueger K, Deissler P, Coburger S, et al. How thrombus model impacts the in vitro study of interventional thrombectomy procedures. *Invest Radiol* 2004; 39: 641–648.
26. Grothues F, Moon JC, Bellenger NG, et al. Interstudy reproducibility of right ventricular volumes, function, and mass with cardiovascular magnetic resonance. *Am Heart J* 2004; 147: 218–223.